Inorganica Chimica Acta 397 (2013) 10–20

Contents lists available at SciVerse ScienceDirect

Inorganica Chimica Acta

journal homepage: www.elsevier.com/locate/ica

A closer look at the formation of bicyclometalated and cyclometalated ruthenium carbonyl complexes

Soumik Mandal [a], Dipravath K. Seth [b], Parna Gupta [a,*]

[a] Department of Chemical Sciences, Indian Institute of Science Education and Research, Kolkata, BCKV Main Post Office, Mohanpur, West Bengal 741252, India
[b] Department of Chemistry, Inorganic Chemistry Section, Jadavpur University, Kolkata 700032, India

ARTICLE INFO

Article history:
Received 4 March 2012
Received in revised form 17 August 2012
Accepted 12 November 2012
Available online 27 November 2012

Keywords:
C–H activation
Ruthenium
Schiff base
Bicyclometalation
Structure elucidation

ABSTRACT

To study steric and electronic factors that affect the C–H activation of Schiff bases by the complex $[Ru(PPh_3)_2(CO)_2Cl_2]$, systematic spectroscopic analyses were performed for a family of Ru(II) complexes of type $[Ru(PPh_3)_2(CO)L]$. Among eight Schiff bases (H_2Ln (n = 1–8)], synthesized by condensation of methyl-4-formyl benzoate with 4-aminoacetophenone, 1-naphthylamine, 2-amino-5-chloropyridine, 8-aminoquinoline, semicarbazide hydrochloride, 2-aminophenol, thiosemicarbazide and 2-aminothiophenol, it was observed that the C–H activation was dependent on the kind as well as the position of the coordinating atoms. The C–H activation of the Schiff bases was most facile in the formation of a Ru-CNO configuration followed by Ru-CNS, Ru-CNN, and Ru-CNC configurations, whereas for a Ru-NC(methine) configuration the activation was the slowest. X-ray crystal structures for five cycloruthenated complexes are reported. Detailed electrochemical studies reveals the redox behavior of the complexes and DFT calculations were performed to obtain geometry optimized structure of all other complexes and to get an insight of the electronic spectral behavior.

1. Introduction

Alkyl or aryl C–H bond cleavage reaction by a ruthenium complex was first reported by Chatt and Davidson in 1965 [1]. Since then, the cyclometalation reaction through C–H activation and cyclometalated complexes continue to be of interest for its application in the synthesis of organic molecules [2–4], particularly in the field of novel materials [5,6] and medicines [7,8]. In these reactions intramolecular C–H activation initiating a cyclometalation reaction has been the key step. Cyclometalation is possible through C–C or C–H eteroatom bond activation. If selective functionalization of alkyl or aryl C–H bonds can be developed, it would have broad application and serve as powerful tool for transformations in organic synthesis. Owing to the easy availability and cost viability, ruthenium complexes are attractive choice for the activation of C–H, C–C and C–N bonds in the alkyl or arene compounds [9–11]. Intuitively it is expected that for ligands with the increase in coordination sites, and with more electronegative atom available for coordination, reaction rates will increase. However, it is not clear whether stable ring formation, electronegativity or steric factor affects the mechanistic pathway significantly or not [12].

To address some of these issues, we have initiated investigations on the C–H activation of some Schiff bases **H_2Ln** or **HLn** by ruthenium(II) where, electronic and steric environment of the ligands were varied significantly [13]. To get an idea of ease of activation of C–H bond, the progress of the reactions were simply monitored by UV-spectroscopy. The reactions of $[Ru(PPh_3)_2(CO)_2Cl_2]$ with ligands H_2Ln (n = **1**,**2**, **5**–**8**, where H stands for dissociable proton) and **HLn** (n = **3** and **4**, where H stands for dissociable proton) (Fig. 1) afforded a group of organoruthenium complexes of composition $[Ru(PPh_3)_2(CO)HL1]$, $[Ru(PPh_3)_2(CO)L4]^+$ (**2**, **3**, **5**–**8**; **L** = **L2**, **L3**, **L5**–**L8**). The reactions, coordination environments and exact molecular structures are shown in Scheme 1. Depending on the proximity of methine or aryl C-atom, only in one of the cases a methine C–H bond (**HL3**) and in all other cases an aryl C–H bond has been activated.

Comparatively rare bicyclometalated ruthenium complex (**2**) has been formed in reaction of **H_2L2** with $[Ru(PPh_3)_2(CO)_2Cl_2]$, where two aryl C–H atoms have been activated [14]. The complexes formed by the reaction of $[Ru(PPh_3)_2(CO)_2Cl_2]$ with the ligands **HL4**, **H_2L5**–**H_2L8** exhibits quite expected coordination mode having CNN(S/O) environment [12,15,16]. Single crystal X-ray study of complex **8** indicates an unprecedented mononuclear cycloruthenated complex of aminothiophenol derived Schiff base.

The present manuscript illustrates the detailed syntheses, spectral and structural characterization, electrochemistry, DFT study and the dependence of the reaction rates for C–H activation with systematic variation of the ligand structure and coordinating atoms.

* Corresponding author. Tel.: +91 3473279130; fax: +91 3473279131.
E-mail address: parna.gupta@gmail.com (P. Gupta).

0020-1693/$ - see front matter © 2012 Elsevier B.V. All rights reserved.
http://dx.doi.org/10.1016/j.ica.2012.11.011

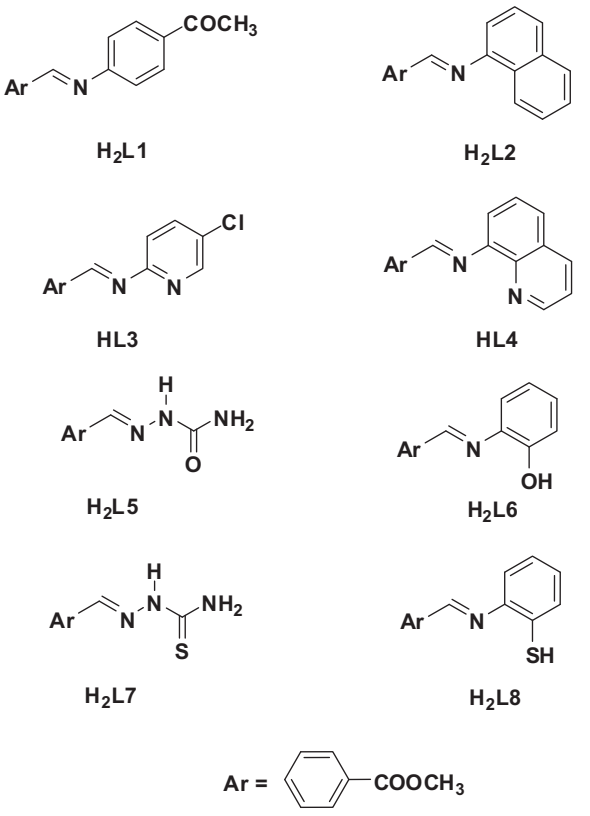

Fig. 1. Molecular structure of ligands H_2L1–H_2L8.

2. Experimental

2.1. Materials

The starting materials $RuCl_3{\cdot}3H_2O$, triphenylphosphane, formaldehyde, KOH, methyl-4-formylbenzoate, p-amino acetophenone, 1-naphthyl amine, 5-chloro-2-aminopyridine, 8-amino quinoline, semicarbazide, 2-aminophenol, thiosemicarbazide, and 2-aminobenzenethiol were purchased from Sigma–Aldrich and used without purification. All the solvents were dried by usual methods prior to use. $[Ru(PPh_3)_2(CO)_2Cl_2]$ were prepared according to the reported procedure [17] and ligand syntheses are given in supporting information.

2.2. Physical measurements

Microanalyses (C, H, N) were performed using a Heraeus Carlo Erba 1108 elemental analyzer. IR spectra were obtained on a Perkin-Elmer Spectrum RXI spectrophotometer with samples prepared as KBr pellets. Electronic spectra were recorded on a U-4100, HITACHI spectrometer. ^{1}H NMR spectra were obtained on a JEOL ECS-400 NMR spectrometer using TMS as the internal standard. Electrochemical measurements were made using a PAR model 273 potentiostat. A platinum disk working electrode, a platinum wire auxiliary electrode and an aqueous Ag/AgCl were used in a three electrode configuration. Electrochemical measurements were made under a dinitrogen atmosphere. All electrochemical data were collected at 298 K and are uncorrected for junction potential. Mass spectra were recorded on a Q-Tof Micromass spectrometer by positive-ion mode electrospray ionization. Optimization of ground-state structures and energy calculations for all the complexes were carried out by density functional theory (DFT) method using the GAUSSIAN 03 package [18], where B3LYP was chosen as the basis function and 6-31g(d,p) basis set was taken for H, C, N, O and Cl and SDD basis set for Ru.

2.3. X-ray crystallography

X-ray diffraction data of five Ru complexes, crystallized mainly by solvent evaporation, were collected on a Bruker SMART APEXII CCD area-detector diffractometer using graphite monochromated Mo Kα radiation (λ = 0.71073 Å). Data reduction included multi-scan corrections for absorption. Structure solution and refinement were done using the SHELXL-TL program package [19]. Selected crystal data and data collection parameters for all the complexes are given in Table 1. Graphic representations of the complexes were generated with program MERCURY [20].

2.4. Synthesis of ruthenium complexes

2.4.1. $[Ru(PPh_3)_2(CO)(HL1)Cl]$ (**1**)

Ligand **H_2L1** (28 mg, 0.10 mmol) along with triethylamine (0.014 mL, 0.10 mmol) was dissolved in toluene (50 mL), refluxed and $[Ru(CO)_2(PPh_3)_2Cl_2]$ (75 mg, 0.10 mmol) was added to the refluxing solution. The reaction mixture was then refluxed for 12 h. The solution was dried under reduced pressure. The resulting light red colored solid was purified by preparative TLC using 14% acetonitrile in toluene (R_f = 0.15) and identity of the complex was confirmed by ESI-MS. Yield: 71 mg (73%); Elemental *Anal.* Calc. for $C_{54}H_{44}ClNO_4P_2Ru$: C, 66.90; H, 4.57; N, 1.44. Found: C, 67.06; H, 4.45; N, 1.63%. ESI-MS (m/z): 935.52 $[M-Cl]^+$; 933.49(M^+-2H); 671.56(M^+-2H-PPh_3); 412.93(M^+-2H-$2PPh_3$); IR (KBr, cm^{-1}): 519, 695, 744(ν_{PPh3}), 1720, 1578($\nu_{C=N}$), 1940(ν_{CO}), 2858, 2928 (ν_{C-H}). ^{1}H NMR (400 MHz, $CDCl_3$, δ ppm); 2,62(s, 3H), 3.96(s, 3H), 7.24–7.27(m, 12H), 7.40(s, 1H), 7.7(d, 2H, J = 8.56 Hz), 7.82(d, 1H, J = 7.86 Hz), 7.98–8.01(m, 18H), 8.15(d, 2H, J = 8.56 Hz), 8.49(s, 1H); ^{13}C NMR(125 MHz, $CDCl_3$, δ ppm): 47.27, 52.36, 111.72, 120.83, 127.00, 128.53, 128.90, 129.44, 129.76, 130.09, 130.76, 132,84, 134.96, 139.44, 143.63, 151.59, 155.76, 160.53, 166.43, 197.18.

2.4.2. $[Ru(PPh_3)_2(CO)(L2)]$ (**2**)

Ligand **H_2L2** (29 mg, 0.10 mmol) and triethylamine (0.028 mL, 0.20 mmol) was dissolved in toluene (50 mL), refluxed and $[Ru(PPh_3)_2(CO)_2Cl_2]$ (75 mg, 0.10 mmol) was added to the boiling solution. The reaction mixture was then refluxed for 2 h. The solution was dried under reduced pressure. The resulting blue solid was purified by preparative TLC using dichloromethane (R_f = 0.5) and identity of the complex was confirmed by ESI-MS and X-ray crystallography. Yield: 75.20 mg (80%). Elemental *Anal.* Calc. for $C_{56}H_{43}NO_3P_2Ru$: C, 71.48; H, 4.61; N, 1.49. Found: C, 70.87; H, 4.34; N, 1.38%. ESI-MS (m/z): 942.32$[M-Cl]^+$; IR (KBr, cm^{-1}): 520, 695, 743 (ν_{PPh3}), 1689, 1716($\nu_{C=N}$), 1927 (ν_{CO}), 2864, 2929(ν_{C-H}); ^{1}H NMR (400 MHz, $CDCl_3$, δ ppm): 3.93(s, 3H), 6.33(d, 1H, J = 7.32 Hz), 6.77(t, 1H, J = 7.32 Hz), 6.87–6.91(m, 2H), 6.96(d, 1H, J = 7.92 Hz), 7.00–7.04(m, 12H), 7.11–7.15(m, 18H), 7.28(s, 1H), 7.36(d, 2H, J = 7.92 Hz), 7.66(d, 1H, J = 6.72 Hz), 8.87(s, 1H); ^{13}C NMR (125 MHz, $CDCl_3$, δ ppm): 51.81, 108.93, 117.98, 121.87, 122.98, 126.28, 126.87, 126.92, 126.97, 127.02, 127.32, 127.70, 128.82, 132.65, 132.86, 133.58, 133.63, 133.68, 146.99, 154.28, 160.93, 168.27.

2.4.3. $[Ru(PPh_3)_2(CO)(L3)Cl]$ (**3**)

Ligand **HL3** (27 mg, 0.10 mmol) along with triethylamine (0.014 mL, 0.10 mmol) was dissolved in toluene (50 mL), refluxed and $[Ru(PPh_3)_2(CO)_2Cl_2]$ (75 mg, 0.10 mmol) was added to the boiling solution. The reaction mixture was then refluxed for 2 h. The solution was dried under reduced pressure and the resulting yellow solid was purified by preparative TLC using toluene (R_f = 0.2)

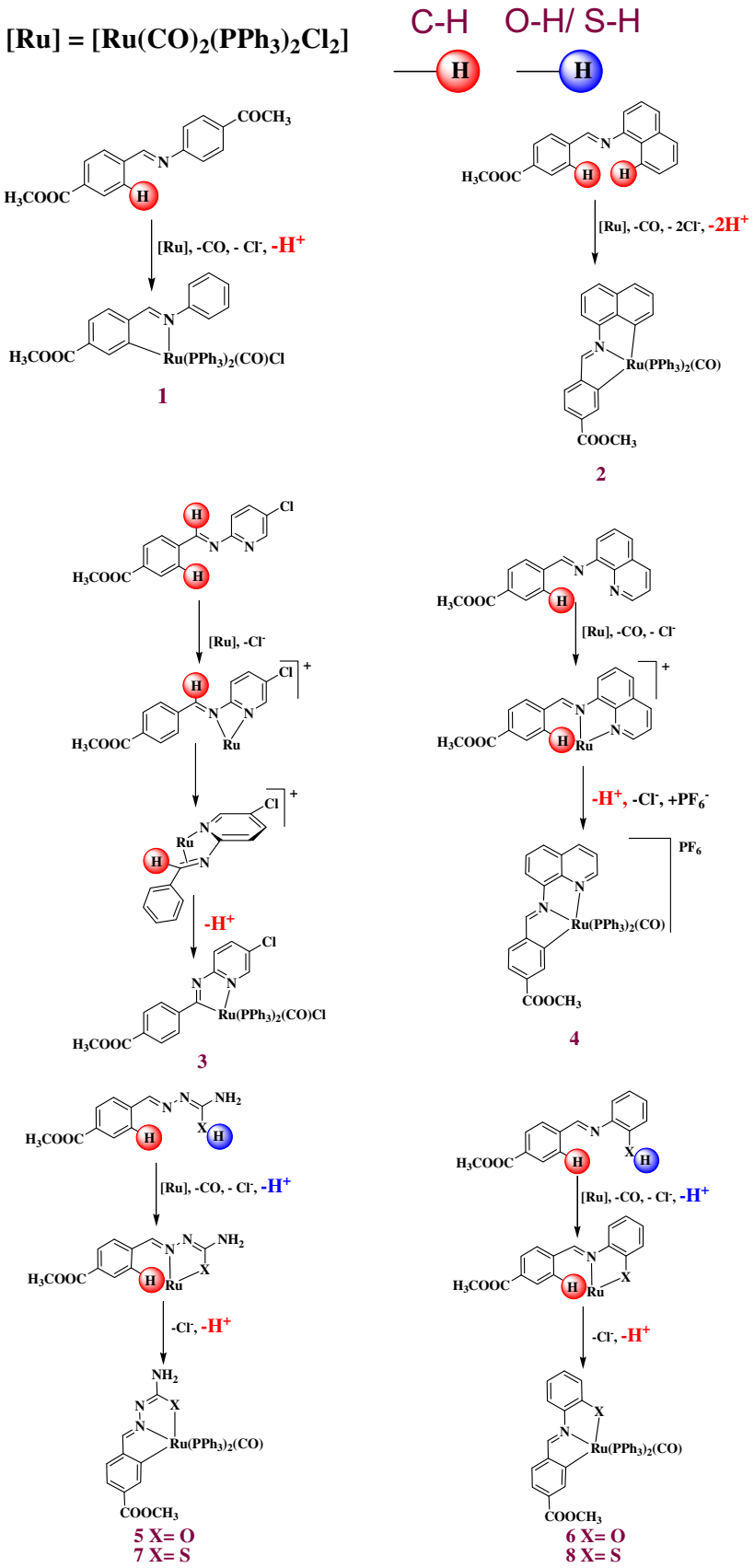

Scheme 1. Probable step for the formation of **1–8**.

Table 1
Crystallographic data for **2·CH$_3$CN**, **3**, **6·C$_2$H$_5$OH**, **7·^{1}/$_2$(CH$_2$OH)$_2$** and **8·CH$_2$Cl$_2$**.

	2·CH$_3$CN	**3**	**6·C$_2$H$_5$OH**	**7·^{1}/$_2$(CH$_2$OH)$_2$**	**8·CH$_2$Cl$_2$**
Empirical formula	$C_{58}H_{46}N_2O_3P_2Ru$	$C_{51}H_{40}Cl_2N_2O_3P_2Ru$	$C_{54}H_{47}NO_5P_2Ru$	$C_{48}H_{42}N_3O_4P_2RuS$	$C_{54}H_{45}Cl_4NO_3P_2RuS$
F.W.	981.98	962.76	952.94	888.91	1092.79
Space group	triclinic, $P\bar{1}$	monoclinic, $P2(1)/c$	triclinic, $P\bar{1}$	triclinic, $P\bar{1}$	monoclinic, $P2(1)/c$
a (Å)	10.1621(19)	11.9613(15)	11.9458(5)	12.6670(9)	13.0091(11)
b (Å)	21.344(4)	29.818(4)	12.9001(6)	12.9370(9)	13.9293(12)
c (Å)	22.796(5)	13.3927(15)	17.0701(8)	13.4361(10)	26.838(2)
α (°)	102.307(4)	90.00	71.556(2)	89.007(4)	90.00
β (°)	96.644(4)	114.918(4)	72.860(2)	68.689(4)	91.268(2)
γ (°)	100.736(4)	90.00	63.978(2)	80.316(4)	90.00
V (Å^3)	4683.7(16)	4332.0(9)	2204.62(17)	2019.7(3)	4862.1(7)
Z	4	4	2	2	4
Crystal, size (mm)	0.43 × 0.11 × 0.03	0.20 × 0.13 × 0.11	0.21 × 0.12 × 0.10	0.21 × 0.12 × 0.10	0.55 × 0.35 × 0.33
Color	blue	yellow	blue	orange	green
T (K)	100	100	100	100	100
μ (mm^{-1})	0.452	0.606	0.480	0.565	0.697
Absorption correction method	multi-scan	multi-scan	multi-scan	multi-scan	multi-scan
Transmission (minimum/maximum)	0.942/0.987	0.910/0.936	0.933/0.953	0.903/0.929	0.746/0.795
Data/parameters	20415/1181	6490/539	9362/571	4186/425	10617/596
θ Range (°)	0.93–27.00	1.81–23.93	1.28–27.00	1.60–20.83	2.11–27.00
$\Delta\rho_{max}$, $\Delta\rho_{min}$	2.737, −1.481	0.639, −0.482	2.538, −1.547	1.470, −0.831	1.805, −1.742
Final R indices [$F^2 > 2\sigma(F^2)$]	R_1 = 0.0552, wR_2 = 0.0978	R_1 = 0.0543, wR_2 = 0.1135	R_1 = 0.0488, wR_2 = 0.1236	R_1 = 0.0664, wR_2 = 0.1810	R_1 = 0.0494, wR_2 = 0.1367
Final R indices (all data)	R_1 = 0.1206, wR_2 = 0.1242	R_1 = 0.0823, wR_2 = 0.1229	R_1 = 0.0650, wR_2 = 0.1309	R_1 = 0.0818, wR_2 = 0.1874	R_1 = 0.0548, wR_2 = 0.1415
Goodness-of-fit	0.999	1.296	1.079	1.289	1.083

and identity of the complex was confirmed by ESI-MS and X-ray crystallography. Yield: 54.24 mg (56%). Elemental *Anal.* Calc. for $C_{51}H_{40}Cl_2N_2O_3P_2Ru$: C, 63.62; H, 4.19; N, 2.91. Found: C, 64.06; H, 4.42; N, 2.80%. ESI-MS (m/z): 927.09 [M−Cl] $^+$; 664.98 (M^+−H-PPh_3); IR (KBr, cm^{-1}): 519, 694, 743 (ν_{PPh3}), 1605, 1716($\nu_{C=N}$), 1936 (ν_{CO}), 2856, 2927(ν_{C-H}); ^{1}H NMR (400 MHz, DMSO-d$_6$, δ ppm): 3.90(s, 3H), 7.24–7.31(m, 12H), 7.37(s, 1H), 7.41(d, 2H, J = 2.76 Hz), 7.64–7.59(m, 18H), 7.78(s, 1H), 7.80(s, 1H), 7.87(d, 2H, J = 2.72 Hz); ^{13}C NMR (125 MHz, DMSO-d$_6$, δ ppm): 109.26, 117.35, 127.00, 128.15, 128.24, 128.70, 128.80, 131.43, 131.52, 132.03, 132.05, 132.31, 133.13, 136.70, 145.63, 158.50, 166.00.

2.4.4. *[Ru(PPh$_3$)$_2$(CO)(L4)](PF$_6$) (**4**)*

Ligand **HL4** (29 mg, 0.10 mmol) and triethylamine (0.014 mL, 0.10 mmol) was dissolved in toluene (50 mL), refluxed and [Ru(CO)$_2$(PPh$_3$)$_2$Cl$_2$] (75 mg, 0.10 mmol) was added to the refluxing

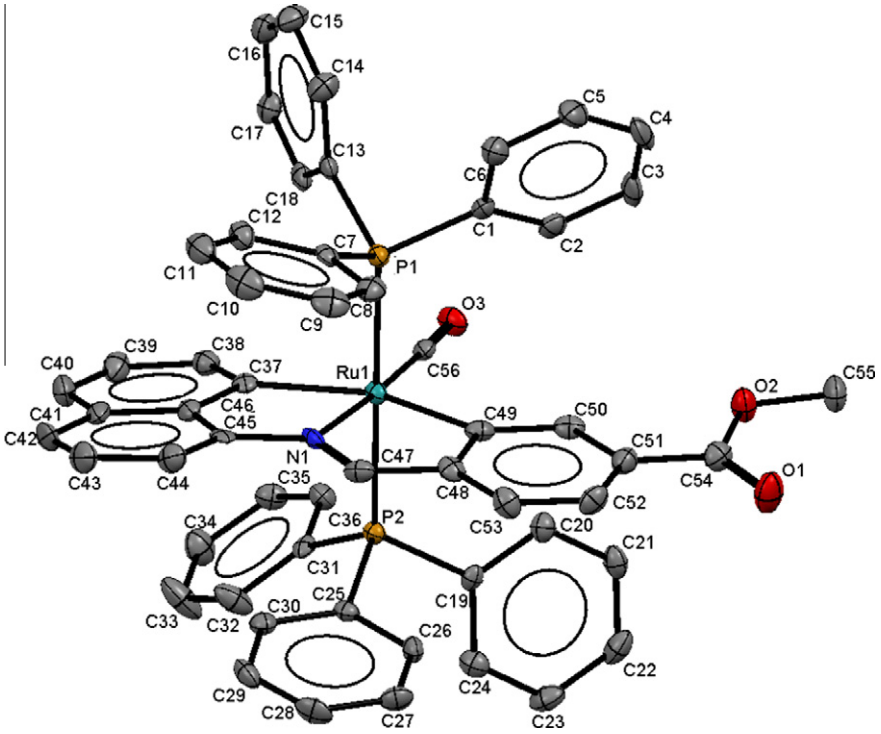

Fig. 2. Molecular structure of **2·CH$_3$CN** with all atoms labeled and thermal ellipsoids at the 50% probability level. Hydrogen atoms and solvent molecule are omitted for clarity.

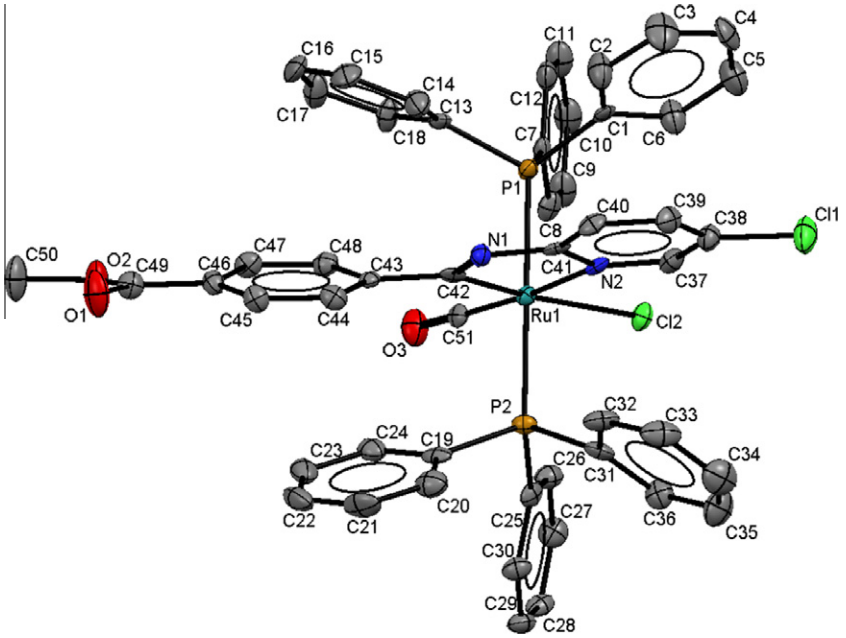

Fig. 3. Molecular structure of **3** with all atoms labeled and thermal ellipsoids at the 50% probability level. Hydrogen atoms are omitted for clarity.

solution. The reaction mixture was then refluxed for 6 h. The solution was dried under reduced pressure and the resulting red colored solid was dissolved in dichloromethane. A methanolic solution of NH_4PF_6 (16.30 mg, 0.10 mmol) was added to the dichloromethane solution, slow evaporation of the solution give red colored precipitate and identity of the complex was confirmed by ESI-MS. Yield: 75.86 mg (70%); Elemental *Anal.* Calc. for $C_{55}H_{44}F_6N_2O_3P_3Ru$: C, 60.66; H, 4.07; N, 2.57. Found: C, 61.06; H, 4.05; N, 2.41%. ESI-MS (m/z): 942.87 $[M-Cl]^+$, 680.87 (M^+−H-PPh_3); IR (KBr, cm^{-1}): 513, 696, 768(ν_{PPh3}), 1702, 1556($\nu_{C=N}$), 1888(ν_{CO}), 2357. ^1H NMR($CDCl_3$, 400 MHz): 3.96(s, 3H), 7.07(t, 3H, J = 7.32 Hz), 7.14–7.18(m, 9H), 7.29–7.32(m, 9H), 7.40(b, 12H), 7.46–7.53(m, 3H), 7.64–7.72(m, 3H), 8.12(s, 1H). ^{13}C NMR($CDCl_3$, 100 MHz): 52.33, 118.28, 118.28, 121.57, 125.58, 126.75, 127.48, 128.07, 128.12, 128.42, 128.48, 128.67, 129.00, 129.13, 129.83, 132.10, 133.52, 133.57, 133.64, 136.12, 136.35, 150.29, 161.63.

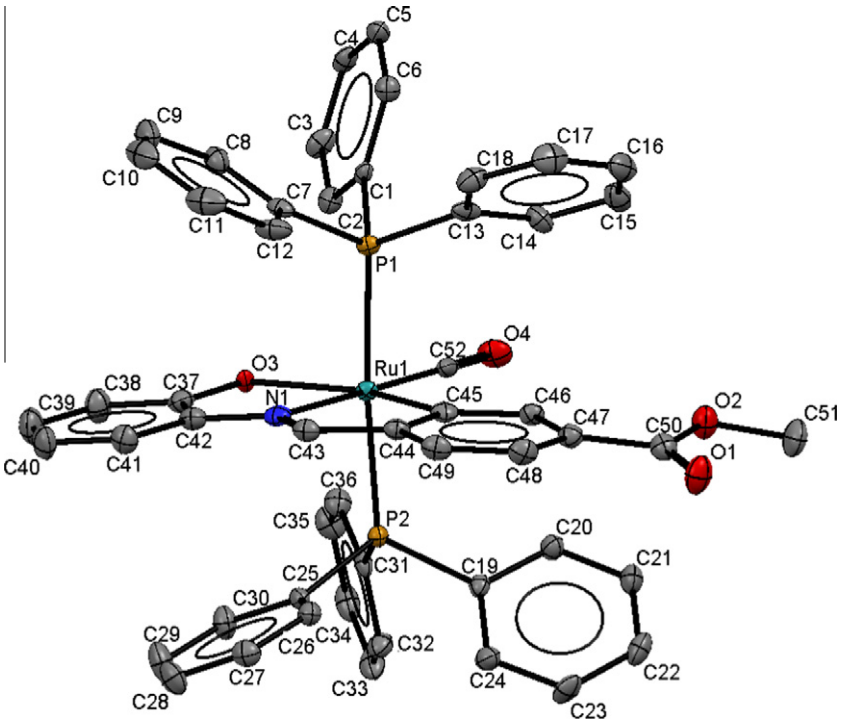

Fig. 4. Molecular structure of **6·C_2H_5OH** with all atoms labeled and thermal ellipsoids at the 50% probability level. Hydrogen atoms and solvent molecule are omitted for clarity.

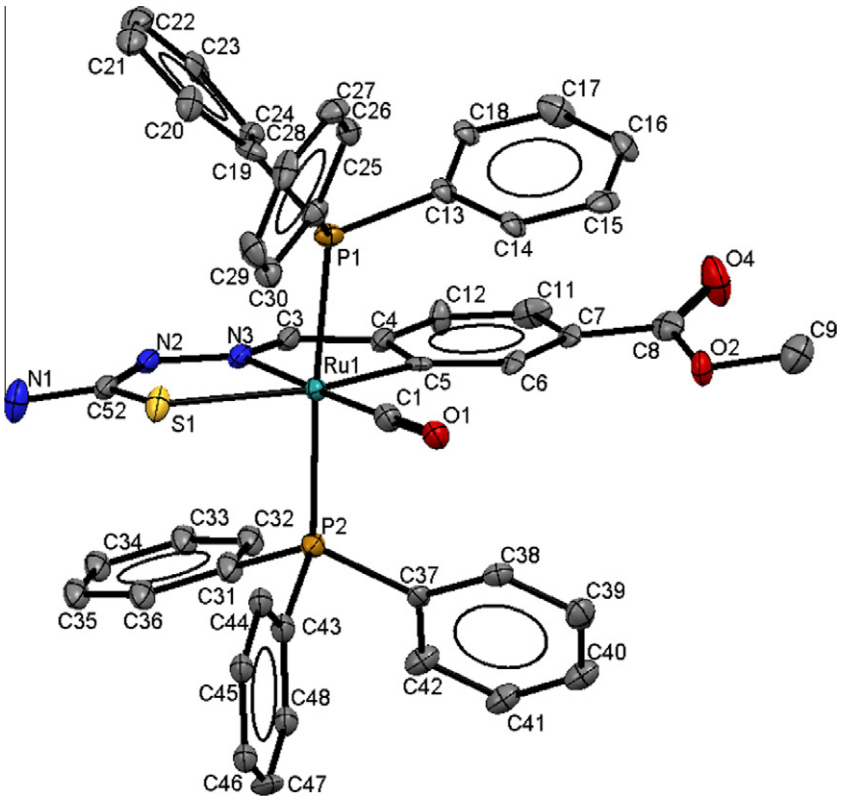

Fig. 5. Molecular structure of **7**·**1/2(CH$_2$OH)$_2$** with all atoms labeled and thermal ellipsoids at the 50% probability level. Hydrogen atoms and solvent molecule are omitted for clarity.

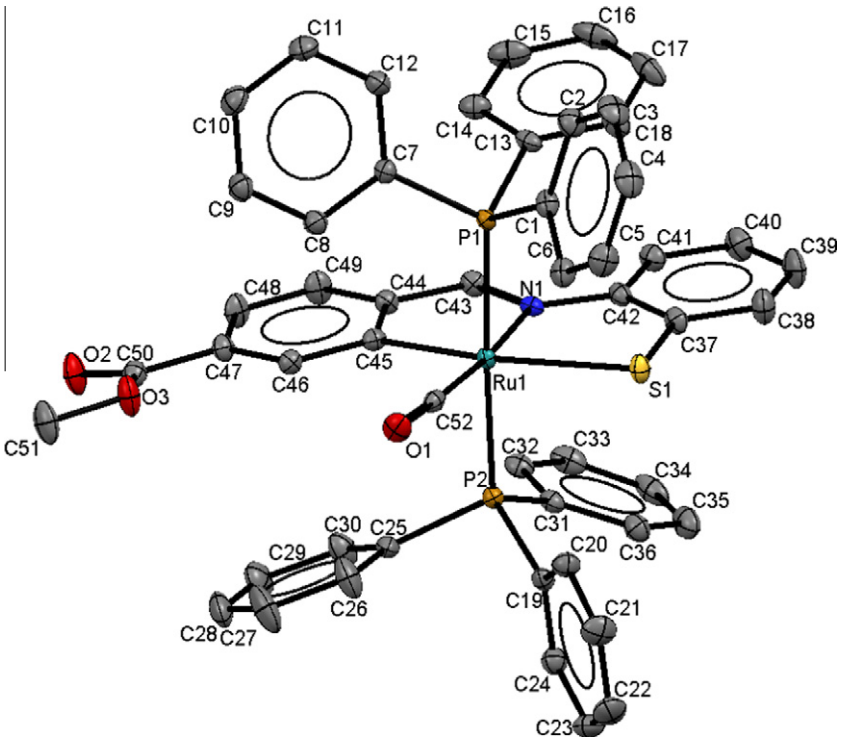

Fig. 6. Molecular structure of **8**·**CH$_2$Cl$_2$** with all atoms labeled and thermal ellipsoids at the 50% probability level. Hydrogen atoms and solvent molecule are omitted for clarity.

Table 2
Key bond lengths (Å) and angles (°) of complexes **2**·CH_3CN, **3**, **6**·C_2H_5OH, **7**·$^1/_2(CH_2OH)_2$, **8**·CH_2Cl_2.

Bond lengths		Bond angles		Bond angles	
2·CH₃CN					
Ru1–P1	2.3618(14)	C56–Ru1–N1	176.14(18)	C112–Ru2–N2	176.37(17)
Ru1–P2	2.3707(13)	C56–Ru1–C49	105.7(2)	C112–Ru2–C93	97.33(19)
Ru1–N1	2.093(4)	N1–Ru1–C49	78.09(17)	N2–Ru2–C93	79.04(17)
Ru1–C37	2.147(5)	C56–Ru1–C37	97.81(19)	C112–Ru2–C105	106.48(18)
Ru1–C49	2.128(5)	N1–Ru1–C37	78.41(17)	N2–Ru2–C105	77.15(16)
Ru1–C56	1.848(5)	C49–Ru1–C37	156.10(19)	C93–Ru2–C105	156.17(18)
Ru2–P3	2.3654(14)	P1–Ru1–P2	177.87(5)	P3–Ru2–P4	175.37(5)
Ru2–P4	2.3828(14)				
Ru2–N2	2.101(4)				
Ru2–C93	2.122(4)				
Ru2–C105	2.165(4)				
Ru2–C112	1.826(5)				
3					
Ru1–P1	2.3818(19)	C51–Ru1–C42	97.9(3)	C51–Ru1–Cl2	98.1(2)
Ru1–P2	2.3907(19)	C51–Ru1–N2	174.0(2)	C42–Ru1–Cl2	164.0(2)
Ru1–Cl2	2.4999(17)	C42–Ru1–N2	76.6(2)	P1–Ru1–P2	177.38(7)
Ru1–N2	2.140(6)	N2–Ru1–Cl2	87.47(15)		
Ru1–C42	2.048(7)				
Ru1–C51	1.829(8)				
6·C₂H₅OH					
Ru1–P1	2.3722(11)	C52–Ru1–C45	100.28(17)	C45–Ru1–O3	156.46(14)
Ru1–P2	2.3808(11)	C52–Ru1–N1	179.63(16)	N1–Ru1–O3	76.78(12)
Ru1–N1	2.082(4)	C45–Ru1–N1	79.70(16)	P1–Ru1–P2	175.14(4)
Ru1–O3	2.228(3)	C52–Ru1–O3	103.25(14)		
Ru1–C45	2.049(4)				
Ru1–C52	1.876(5)				
7·$^1/_2(CH_2OH)_2$					
Ru1–P1	2.388(3)	C1–Ru1–C5	97.4(5)	C5–Ru1–S1	156.3(3)
Ru1–P2	2.375(3)	C1–Ru1–N3	176.3(5)	N3–Ru1–S1	77.4(3)
Ru1–S1	2.467(3)	C5–Ru1–N3	78.9(4)	P2–Ru1–P1	175.14(12)
Ru1–N3	2.119(9)	C1–Ru1–S1	106.3(4)		
Ru1–C1	1.830(13)				
Ru1–C5	2.092(11)				
8·CH₂Cl₂					
Ru1–P1	2.3728(9)	C52–Ru1–C45	94.27(14)	C45–Ru1–S1	160.09(10)
Ru1–P2	2.3619(9)	C52–Ru1–N1	173.31(13)	N1–Ru1–S1	81.34(8)
Ru1–N1	2.113(3)	C45–Ru1–N1	79.07(12)	P2–Ru1–P1	177.43(3)
Ru1–S1	2.4591(9)	C52–Ru1–S1	105.34(10)		
Ru1–C45	2.064(3)				
Ru1–C52	1.844(3)				

*2.4.5. [Ru(PPh$_3$)$_2$(CO)L5] (**5**)*

Ligand **H_2L5** (22 mg, 0.10 mmol) was dissolved in toluene (50 mL), triethylamine (0.014 ml, 0.10 mmol) was added. The resulting solution was refluxed and [Ru(CO)$_2$(PPh$_3$)$_2$Cl$_2$] (75 mg, 0.10 mmol) was added. The reaction mixture was refluxed for 2 h. The solution was dried under reduced pressure and the resulting light orange colored solid was purified by preparative TLC using 20% acetonitrile in toluene (R_f = 0.6) and identity of the complex was confirmed by elemental analysis and ESI-MS. Yield: 49.57 mg (57%); Elemental *Anal.* Calc. for $C_{47}H_{40}N_3O_4P_2Ru$: C, 64.67; H, 4.61; N, 4.81. Found: C, 64.93; H, 4.54; N, 4.65%. ESI-MS (*m*/*z*): 874.08 [M−Cl]$^+$; IR (KBr, cm^{-1}): 516, 693, 769(ν_{PPh3}), 1698, 1578($\nu_{C=N}$), 1727(ν_{CO}), 2858, 2928(ν_{C-H}), 3180(ν_{N-H}); ^{1}H NMR (400 MHz, $CDCl_3$, δ ppm); 3.34(s, 3H), 5.22(s, 2H) 7.90–8.10(m, 32H), 8.30(s, 1H), 9.19(s, 1H), 10.95(s, 1H); ^{13}C NMR (125 MHz, $CDCl_3$, δ ppm): 52.22, 127.14, 127.63, 128.24, 128.46, 128.55, 129.87, 131.96, 132.05, 132.13, 132.30, 132.86, 133.95, 134.11, 166.51.

*2.4.6. [Ru(PPh$_3$)$_2$(CO)L6] (**6**)*

Ligand H_2L6 (26 mg, 0.10 mmol) was dissolved in toluene (50 mL), triethylamine (0.014 mL, 0.10 mmol) was added, refluxed and [Ru(CO)$_2$(PPh$_3$)$_2$Cl$_2$] (75 mg, 0.10 mmol) was added to the refluxing solution. The reaction mixture was then refluxed for 2 h. The greenish yellow solution was dried under reduced pressure and the resulting blue solid was purified by TLC using 10% acetonitrile in toluene (R_f = 0.25) and identity of the complex was confirmed by ESI-MS and X-ray crystallography. Yield: 80.48 mg (89%). Elemental *Anal.* Calc. for $C_{52}H_{42}NO_4P_2Ru$: C, 68.79; H, 4.66; N, 1.54. Found: C, 67.98; H, 5.02; N, 1.47%. ESI-MS (*m*/*z*): 906.63 [M−Cl]$^+$; IR (KBr, cm^{-1}): 518, 694, 770(ν_{PPh3}), 1715, 1588($\nu_{C=N}$), 1934(ν_{CO}), 2851, 2922(ν_{C-H}). ^{1}H (400 MHz, $CDCl_3$ δ ppm): 3.90(s, 3H), 7.22–7.35(m, 18H), 7.46–7.50(m, 4H), 7.62(d, 2H, *J* = 8.72 Hz), 7.99–8.18(m, 12H), 8.33(s, 1H), 8.35(s, 1H). ^{13}C NMR (125 MHz, $CDCl_3$, δ ppm): 30.61, 52.51, 65.90, 111.08, 125.11, 126.10, 127.54, 127.89, 129.34, 129.50, 129.60, 129.98, 130.35, 132.12, 133.32, 133.41, 141.35, 150.33, 165.49, 192.85.

*2.4.7. [Ru(PPh$_3$)$_2$(CO)L7] (**7**)*

Ligand H_2L7 (24 mg, 0.10 mmol) was dissolved in toluene (50 mL), triethylamine (0.014 mL, 0.10 mmol) was added, refluxed and [Ru(CO)$_2$(PPh$_3$)$_2$Cl$_2$] (75 mg, 0.10 mmol) was added to the boiling solution. The reaction mixture was then refluxed for 2 h. The solution was dried under reduced pressure and the resulting orange solid was purified by preparative TLC using 5% acetonitrile in toluene (R_f = 0.2) and identity of the complex was confirmed by ESI-MS and X-ray crystallography. Yield: 66.58 mg (75%); Elemental *Anal.* Calc. for $C_{47}H_{40}N_3O_3P_2RuS$: C, 63.43; H, 4.53; N, 4.72. Found: C, 63.24; H, 4.43; N, 4.62%. ESI-MS (*m*/*z*): 889.91 [M−Cl]$^+$; IR (KBr, cm^{-1}): 516, 693, 769(ν_{PPh3}), 1698, 1578($\nu_{C=N}$),

Table 3
Selected orbital contribution of complexes **1**–**8**.

Complex	Contributing fragments	%Contribution of fragments to	
		HOMO	LUMO
1	Ru	35.62	15.04
	Cl	46.32	6.41
	CO	10.86	5.26
	L1	6.46	72.61
	PPh_3	0.74	0.68
2	Ru	56.28	8.13
	CO	5.18	1.53
	L2	38.75	89.63
	PPh_3	0.79	0.71
3	Ru	36.16	11.26
	Cl	43.75	3.21
	CO	4.37	1.29
	L3	15.05	83.62
	PPh_3	0.67	0.62
4	Ru	55.58	12.58
	CO	2.43	5.23
	L4	41.17	81.44
	PPh_3	0.82	0.75
5	Ru1	58.10	5.32
	CO	3.71	16.67
	L5	37.46	77.36
	PPh_3	0.73	0.65
6	Ru1	52.98	5.78
	CO	3.06	8.02
	L6	43.33	85.66
	PPh_3	0.63	0.54
7	Ru1	58.36	5.97
	CO	2.23	8.89
	L7	5.78	84.65
	PPh_3	0.54	0.49
8	Ru1	45.21	4.96
	CO	2.44	7.78
	L8	12.39	86.69
	PPh_3	0.78	0.57

1921(ν_{CO}), 2858, 2928(ν_{C-H}), 3255(ν_{N-H}); ^{1}H NMR (400 MHz, $CDCl_3$, δ ppm): 3.84(s, 3H), 4.57(d, 2H, J = 6.32 Hz), 7.1–7.6(m, 32H), 7.91(s, 1H), 7.93(s, 1H); ^{13}C NMR (125 MHz, $CDCl_3$, δ ppm): 51.94, 62.33, 126.28, 127.93, 128.68, 128.77, 129.00, 129.54, 129.75, 131.40, 131.49, 132.00, 133.10, 148.40, 166.21.

*2.4.8. [Ru(PPh$_3$)$_2$(CO)L8] (**8**)*

Ligand **H_2L8** (27 mg, 0.10 mmol) was dissolved in toluene (50 mL), triethylamine (0.014 mL, 0.10 mmol) was added, refluxed and [Ru(CO)$_2$(PPh$_3$)$_2$Cl$_2$] (75 mg, 0.10 mmol) was added to the boiling solution. The reaction mixture was then refluxed for 2 h. The solution was concentrated under reduced pressure and the resulting orange solid was purified by preparative TLC using dichloromethane in toluene (R_f = 0.4) and identity of the complex was confirmed by ESI-MS and X-ray crystallography. Yield: 78.68 mg (85%); Elemental *Anal.* Calc. for $C_{52}H_{42}NO_3P_2RuS$: C, 67.59; H, 4.58; N, 1.52. Found: C, 67.57; H, 4.43; N, 1.52%. ESI-MS (m/z): 922.82 $[M-Cl]^+$; IR (KBr, cm^{-1}): 528, 682, 728(ν_{PPh3}), 1710, 1564($\nu_{C=N}$), 1904(ν_{CO}), 2893, 2947(ν_{C-H}). ^{1}H NMR (400 MHz, $CDCl_3$, δ ppm): 3.83(s, 3H), 5.91(d, 1H, J = 7.92 Hz), 6.07(t, 1H, J = 6.72 Hz), 6.37(t, 1H, J = 7.32 Hz), 6.55(d, 1H, J = 7.96 Hz), 6.94(d, 1H, J = 7.96 Hz), 7.09–7.18(m, 18H), 7.25(t, 1H, J = 7.32 Hz), 7.34–7.39(m, 1H), 7.44–7.50(m, 12H), 7.80(s, 1H); ^{13}C NMR(100 MHz, DMSO-d_6, δ ppm): 51.74, 116.16, 121.56, 127.37, 127.41, 127.45, 128.39, 128.84, 129.51, 132.26, 132.48, 132.70, 133.47, 133.52, 133.56, 142.02, 143.56, 153.04, 153.28, 166.60.

3. Results and discussion

Reaction of potentially [C,N,X], (X = O, S, N, C) terdentate Schiff bases (**H_2L1**–**H_2L8**) with [Ru(PPh$_3$)$_2$(CO)$_2$Cl$_2$] in refluxing toluene afforded a group of cyclometalated complexes (**1**–**8**) in moderate yield. To envisage the C–H activation of the ligands by [Ru(PPh$_3$)$_2$(CO)$_2$Cl$_2$], extensive spectral and structural studies were done with the resulting ruthenium complexes. The complexes described in this paper were characterized by elemental analysis, IR spectroscopy, ^{1}H and ^{13}C{^{1}H} NMR spectroscopy, ESI-MS and X-ray crystallography. As we are interested in C–H activation, one methine or aryl carbon atom was kept in the vicinity of the ruthenium. The ruthenium(II) has successfully activated methine or aryl C–H bond to form metal–carbon(sp^{2}C) σ-bond in every complex (Scheme 1). The ligands coordinate Ru in terdentate fashion, except for [Ru(PPh$_3$)$_2$(CO)(HL1)Cl] (**1**) and [Ru(PPh$_3$)$_2$(CO)(L3)Cl] (**3**). Two aryl C–H bonds have been activated to generate bicyclometalated ruthenium(II) complex [Ru(PPh$_3$)$_2$(CO)(L2)Cl] (**2**). The compositions of the complexes were confirmed by elemental analyses, ESI-MS as well as structures of the complexes **2·CH$_3$CN**, **3**, **6·C$_2$H$_5$OH**, **7·^{1}/$_2$(CH$_2$OH)$_2$**, **8·CH$_2$Cl$_2$** were determined by single crystal X-ray diffraction. The structures are shown in Figs. 2–6 and selected bond parameters are presented in Table 2.

The complexes (**1**–**8**, Scheme 1) have one carbonyl and two triphenylphosphanes attached to the ruthenium center and all of them have the P1–Ru–P2 angle around 180 ± 3° [21]. The average Ru–P (2.3758 Å) and Ru–CO (1.8468 Å) bond lengths are quite normal and comparable with similar type of complexes of ruthenium(II) [17]. The average Ru–C (methine or aryl) distance (2.0607 Å) is quite normal for **3**, **6**–**8** [15,22,23], but a little longer in case of **2** [14].

Treatment of [Ru(PPh$_3$)$_2$(CO)$_2$Cl$_2$] with **H_2L1** and **H_2L2** and subsequent purification results in the formation of **1** and **2**. The elemental analysis, ESI-MS and NMR spectroscopic data clearly indicate that the **H_2L1** is κ^2-C,N bonded [22,23] to the ruthenium center in case of **1** and the expected composition of synthesized complex is [Ru(PPh$_3$)$_2$(CO)(HL1)Cl]. ESI-MS of **1** (Fig. S1) shows molecular ion peak at m/z 935.52(M^+) attributable to [Ru(PPh$_3$)$_2$(CO)(HL1)]$^+$. Geometry optimized structure of **1** (Fig. S2) has been obtained using DFT calculation as good quality single crystal could not be grown. Obtained bond parameters are given in Table S1. An interesting bicyclometalated complex has formed, when [Ru(PPh$_3$)$_2$(CO)$_2$Cl$_2$] reacts with **H_2L2**, where, both benzene and napthyl ring C–H have been activated. Molecular structure of **2** (Fig. 2) shows monomeric compound in which ruthenium sits in the center of a distorted octahedron, coordinated to C(37), C(49) and N1(imine nitrogen) of dianionic tridentate **L2**. The fourth coordination site in the equatorial plane is occupied by carbonyl C(56). Extensive literature survey could not find any single example of bicyclometalated complex like **2** [14]. The angles around the ruthenium center deviate significantly from 90°. The angles C56–Ru1–C49, C56–Ru1–C37 opened up to 105.7(2), and 97.81(19) whereas, N1–Ru1–C49 and N1–Ru1–C37 angles have reduced to 78.09(17), 78.41(17). Moreover, the C49–Ru1–C37 angle of 156.10(19) suggests significant distortion from octahedral geometry.

The X-ray crystal structure of **3** (Fig. 3) reveals that ligand **HL3** is coordinated to six-coordinated ruthenium center as **L3**, through pyridine-N and the iminoacyl-carbon to form a stable five-membered chelate with a C39–Ru1–N1 angle of 76.58°(19). The ruthenium has a C_2NP_2Cl coordination sphere in this complex. The ligand **L3**, ruthenium, carbonyl and chloride constitute the equatorial plane of the octahedron with the metal at the center, and as mentioned earlier, two triphenylphosphane ligands take up the two axial positions. The carbonyl lie *trans* to the pyridine(py) nitrogen atom of the py–N=CHAr (**L3**) and the chloride is *trans* to the

Table 4
Electrochemical and electronic spectral data of complexes **1**–**8**.

Complex	Electronic spectral data λ_{max}, nm ($\epsilon \times 10^{-4}$, $M^{-1}cm^{-1}$)[a]	Cyclic voltammetric data[b], *E*, V vs. SCE
1	378(0.77), 315[c](8.5)	1.24[f], 1.04[f], −1.37[g]
2	524(0.17), 379(0.50)	0.903[f], −1.224[g], −1.644[g]
3	403(0.21), 310[c](0.85)	1.04, 1.39, −1.11[g], −1.60[g]
4	560(0.24), 376(0.72), 325(1.56), 288[c](2.10)	0.685, 1.22, −0.99[g]
5	324(2.20)	0.51[d](80)[e], 0.71[f], −.03[g], −1.44[d](70)[e]
6	594(0.086), 471(0.091), 409(0.23), 371[c](0.37)	0.58[d](70)[e], 1.30[f], −1.15[g], −1.59[g]
7	464(0.057), 357(0.37), 290(1.10)	0.65[d](80)[e]1.18[f], −1.04[g]
8	419[c](0.43), 373(0.93), 297(0.32)	0.36(70), 0.693, 1.22[f], −1.65[g]

[a] Dichloromethane solution.
[b] Dichloromethane/acetonitrile (1:9), TBAP supporting electrolyte.
[c] Shoulder.
[d] $E_{1/2} = 0.5(E_{pa} + E_{pc})$, where E_{pa} and E_{pc} are anodic and cathodic peak potentials, respectively, scan rate 50 mV s^{-1}.
[e] $\Delta Ep = E_{pa} - E_{pc}$ in mV.
[f] E_{pa} value.
[g] E_{pc} value.

imine carbon (N=C) atom. All bond lengths are in the expected limit, except Ru–N and Ru–Cl bonds [21,24,25], which are a little longer, may be due to the presence of two *trans*-PPh_3 ligands. Earlier report by Kirchner group [26,27] shows ligand with coordination environment similar to **HL3**, provides either κ^2-N,N-coordinated or aminocarbene ruthenium complexes, where the Ru–C bond length varies from 1.83 to 1.93 Å [13]. However, an interesting coordination mode of py–N=CHAr (**HL3**) with ruthenium is being revealed here with Ru–C bond length of (2.045(5) Å), indicating the presence of metal–carbon σ-bond. They have proposed that steric restrictions and presence of strongly π-accepting PPh_3, CO ligands prevent an oxidative addition step in the formation of κ^2-N,C coordinated complex. Presence of PPh_3 and CO together, due to strong π-accepting character and steric factor, probably prevents the formation of ruthenium carbene and facilitates the formation of more stable five-membered iminoacyl ruthenium complex. Reaction of **HL4** with $[Ru(PPh_3)_2(CO)_2Cl_2]$ generate cationic complex **4** with $C_2N_2P_2$ (Scheme 1) coordination environment, where ligand provides tridentate NNC coordinating environment. The complex has precipitated out from the solution as PF_6-salt. Lack in quality of the single crystal prevented further detailed structural studies of this complex. Composition of the complex was confirmed by elemental analysis, ESI-MS (Fig. S3) and NMR studies. Geometry optimized structure (Fig. S4) has been obtained from DFT study and bond parameters are given in Table S1.

Ligands **H_2L5**–**H_2L8**, on reaction with $[Ru(PPh_3)_2(CO)_2Cl_2]$, affords mononuclear complexes where the ligand bind as tridentate κ^3-C,N,O/S (Scheme 1), replacing two chloride and one carbonyl from the ruthenium precursor. The structural studies on $[Ru(PPh_3)_2(CO)L6]$ (**6**) (Fig. 4), $[Ru(PPh_3)_2(CO)L7]$ (**7**) (Fig. 5) and $[Ru(PPh_3)_2(CO)L8]$ (**8**) (Fig. 6) confirm that six-coordinated ruthenium center bound to one dianionic tridentate CNO/S-donor ligand, one carbonyl, and two axial triphenylphosphanes. ESI-MS and geometry optimized structure of **5**, is shown in Figs. S5 and S6, respectively. Extensive study by Bhattacharya group [12,15] on the possible coordination mode of the benzaldehyde semicarbazone and thiosemicarbazones reveals that, formation of five-membered chelate ring is difficult but possible for these ligands, as they have a rigid geometry across the C=N bond. But, *ortho*-metalation of the pendant phenyl ring by C–H bond activation under suitable reaction condition is possible. The crystal structure of **7** (Fig. 5) shows that, the thiosemicarbazone ligand gets coordinated to ruthenium as an CNS(anionic) donor. The Ru–S bond length is 2.469(3) comparable [15]. The geometry around the ruthenium in complexes 6 and **8** are similar, only oxygen (**6**) is being replaced by sulfur (**8**). Though complexes with similar coordination pattern to **6** is available in literature [28], no report of complex similar to **8** is available in the literature. This is the first ever report of cycloruthenated complex coordinated to anionic sulfur attached to an aromatic ring. The Ru–S bond [Ru1–S1 2.4591(9)] is comparable to the Ru–S bond in complex **7**.

Infrared spectra of all the complexes show multiple bands of varying intensities within the range 4000 to 400 cm^{-1}. The metal–carbon stretching band in the region 740–800 cm^{-1} cannot be assigned from the spectra, because of overlap by strong triphenylphosphane bands. Three strong bands observed around 520, 695, 730–770 and 1940 cm^{-1} in all the complexes are attributable to the coordinated triphenylphosphanes and carbonyl respectively, for all the complexes. The bands at around 1570 and 1700 cm^{-1} (**2**–**6**) are due to $\nu_{C=N}$ which were absent in the precursor complex.

Each complex shows several intense absorptions in the visible and UV region. The absorptions in the UV region are believed to be due to transitions within the ligand orbitals. In order to assign the lowest energy absorption in the visible region, DFT (**1**–**8**) and TD-DFT (**1**, **3**) calculations were performed using the crystallographic coordinates (for complex **2**, **3**, **6**, **7**, **8**). Selected orbital contribution of all the complexes are given in Table 3. It is interesting to note that, for the complexes **1** and **3**, coordinated chloride ligand has considerable contribution in highest occupied molecular orbital (HOMO). Because of the mixed Ru d(π)–Clp(π) character of the HOMO, a mixed MLCT/XLCT character of the transition is inaccurate because of the delocalised character of the relevant orbitals. This assignment proposed [29], with the Cl to **HL1** or **L3** XLCT contribution prevailing. Of course this description is further supported by the following comparison. The absorption spectrum of **1** closely resembles that of **3** (see Table 4). In case of all other complexes (**2**, **4**–**8**), HOMO holds maximum contribution from metal center and LUMO possesses predominant ligand contribution. Hence, we assign the lowest absorption band in the spectra to this HOMO → LUMO transition, which can be best be viewed as σ_{metal}–π^*_L transition. The other absorptions in the visible region are attributable to transitions occurring from the ruthenium t_2 orbitals to the higher energy vacant orbitals. The absorptions in the UV region are due to transitions within the ligand orbitals. Frontier orbital surface diagram of complexes **3** and **4** are shown in Fig. 7.

To get an idea regarding the oxidation and reduction processes, the complexes have been studied by cyclic voltammetry in 1:9 dichloromethane–acetonitrile solution (0.1 M TBAP) and voltammetric data are presented in Table 4. Each of the complexes shows one to two oxidative and reductive responses. The origin of reduction and oxidation are assigned from the HOMO and LUMO population. For the complexes **1** and **3**, there occurs halogen mediated metal oxidation, as HOMO posses mixed chloride and metal

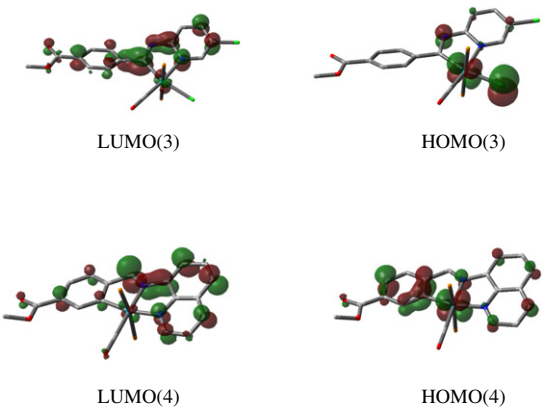

Fig. 7. Contour plots of HOMO and LUMO of the complexes **3** and **4** (hydrogen atoms are omitted for clearity).

Table 5
Time to complete the formation of ruthenium complexes **1**–**8**.

Complex	Time of completion (min)
1	850
2	651
3	31
4	198
5	37
6	15
7	32
8	71

character. Since the metal contribution is predominant in the HOMO of all other six complexes, first oxidation is assigned to metal oxidation. The reductive response arose are due to imine-ligand reduction. The first oxidative response is irreversible in nature for complexes **1**–**4**, whereas, for **5**–**8** it is reversible in nature characterized by a peak-to-peak separation (ΔEp) of 70–80 mV. The irreversible reductive response observed around 1.0–1.1 V may be assigned to reduction of the imine fragment in the coordinated ligands.

To study the C–H activation of **H_2L1**–**H_2L8** by ruthenium(II), a very simple experiment has been done. The time required for completion and the changes in the UV–vis spectrum with time during the reaction of $[Ru(PPh_3)_2(CO)_2Cl_2]$ with ligands **H_2L1**–**H_2L8** were plotted (Fig. S7). The time required for completion of the reactions has been tabulated in Table 5. For the sake of our study, reaction parameters like solvent, solvent volume, concentration and temperature were kept constant. The slowest rate of formation of complex is observed with **H_2L1**, where single aryl C–H bond has been activated and the ligand binds to the metal center in bidentate fashion. Except, rate of formation of **1**, **2** and **4**, all other reactions are quite fast and comparable. The plausible mechanism for every case was suggested in Scheme 1. The closer look at the time of completion suggests that the aryl C–H activation is the second and rate determining step of the reactions and the initial binding of metal to aryl carbon(along with imine nitrogen), in case of **1** and **2** render the reactions slow. In all other cases, the initial binding to N/O/S present in the ligand along with imine nitrogen brings the pendent phenyl ring closer to the metal center to make the otherwise difficult C–H bond activation easier. This is not applicable for **4** and the unusual rate of formation of complex **4** is due to difficulty in releasing the H^+ from a cationic species. Definitely, stable chelate ring formation is one of the most important criteria of the metal–ligand complex formation and that too, is reflected in formation of complex **3**. If, metal center prefers to coordinate the more electronegative atom over carbon, we should end up at a four-membered cationic complex as **3**. It is significant to note that, electronic and steric environment along with the stable ring formation directs the bonding pattern as well as control the rate of the reaction.

4. Conclusions

The present study shows that a series of Schiff base ligands (**H_2L1**–**H_2L8**) can undergo facile C–H activation mediated by $[Ru(PPh_3)_2(CO)_2Cl_2]$ under mild reaction condition. The experimental condition helps to activate both the acyl C–H and aryl C–H bond. The C–H bond activation of ligands with varying coordination environment, were studied by a simple experiment. The synthesis, reactivity and kinetic study reported here will definitely provide useful insight for the templated designing of organic molecule through C–H activation. Further study in this direction is presently being carried out in our laboratory.

Acknowledgments

P.G. would like to thank the Department of Science and Technology, India, Research Grant SR/FT/CS-057/2009 and IISER Kolkata central XRD facility. S.M. and D.K.S. thank the CSIR, India for financial support. Authors are grateful to Prof. Samaresh Bhattacharya, Jadavpur University, Dr. Indranil Bhattacharyya, ND College, Howrah for their help.

Appendix A. Supplementary data

CCDC 841461, 821627, 821629, 821628 and 842508 contain the supplementary crystallographic data for complexes **2·CH_3CN**, **3**, **6·C_2H_5OH**, **7·$^1/_2(CH_2OH)_2$** and **8·CH_2Cl_2**, respectively. These data can be obtained free of charge from The Cambridge Crystallographic Data Centre via http://www.ccdc.cam.ac.uk/data_request/cif. Supplementary data associated with this article can be found, in the online version, at http://dx.doi.org/10.1016/j.ica.2012.11.011.

References

[1] J. Chatt, J.M. Davidson, J. Chem. Soc. (1965) 843.
[2] S. Murahashi, Ruthenium in Organic Synthesis, Wiley, New York, 2004.
[3] T. Naota, T. Hikaru, S. Murahashi, Chem. Rev. 98 (1998) 2599.
[4] G. Dyker, Handbook of C–H Transformations: Applications in Organic Synthesis, Wiley, New York, 2000.
[5] G. van Koten, R.J.M.(Bert)K. Gebbink, Dalton Trans. 40 (2011) 8731.
[6] M.E. van der Boom, D. Milstein, Chem. Rev. 103 (2003) 1759.
[7] R. Anand, J. Maksimoska, N. Pagano, E.Y. Wong, P.A. Gimotty, S.L. Diamond, E. Meggers, R. Marmorstein, J. Med. Chem. 52 (2009) 1602.
[8] N.B. Johnson, I.C. Lennon, P.H. Moran, J.A. Ramsden, Acc. Chem. Res. 40 (2007) 1291.
[9] G.C. Vougioukalakis, R.H. Grubbs, Chem. Rev. 110 (2010) 1746.
[10] S.I. Murahashi, H. Takaya, Acc. Chem. Res. 33 (2000) 225.
[11] C. Gunanathan, D. Milstein, Acc. Chem. Res. 44 (2011) 588.
[12] F. Basuli, S.M. Peng, S. Bhattacharya, Inorg. Chem. 40 (2001) 1126.
[13] H.A. Zhong, J.A. Labinger, J.E. Bercaw, J. Am. Chem. Soc. 124 (2002) 1378.
[14] X.W. Li, F. Chen, W.F. Xu, Y.Z. Li, X.T. Chen, Z.L. Xue, Inorg. Chem. Commun. 14 (2011) 1673.
[15] S. Dutta, F. Basuli, A. Castineiras, S.M. Peng, G.H. Lee, S. Bhattacharya, Eur. J. Inorg. Chem. 29 (2008) 4538.
[16] L.R. Hanton, T. Kemmitt, Chem. Commun. 10 (1991) 700.
[17] A. Ahmed, S.D. Robinson, M.F. Uttley, J. Chem. Soc., Dalton Trans. 7 (1972) 843.
[18] A.D. Becke, J. Chem. Phys. 98 (1993) 5648.
[19] G.M. Sheldrick, Acta. Crystallogr., Sect. A 64 (2008) 112.
[20] C.F. Macrae, I.J. Bruno, J.A. Chisholm, P.R. Edgington, P. McCabe, E. Pidcock, L. Rodriguez-Monge, R. Taylor, J. van de Streek, P.A. Wood, J. Appl. Crystallogr. 41 (2008) 466.
[21] S. Nag, P. Gupta, R.J. Butcher, S. Bhattacharya, Inorg. Chem. 43 (2004) 4814.
[22] K. Ghosh, S. Kumar, R. Kumar, U.P. Singh, N. Goel, Inorg. Chem. 49 (2010) 7235.

[23] W.R. Roper, L.I. Wright, J. Organomet. Chem. 142 (1977) Cl.
[24] K. Omura, T. Uchida, R. Irie, T. Katsuki, Chem. Commun. 18 (2004) 2060.
[25] C.G. Roy, S.S. Sen, S. Dutta, G. Mostafa, S. Bhattacharya, Polyhedron 26 (2007) 3876.
[26] C.M. Standfest-Hauser, K. Mereiter, R. Schmid, K. Kirchner, Organometallics 21 (2002) 4891.
[27] C. Slugovc, K. Mereiter, R. Schmid, K. Kirchner, Organometallics 17 (1998) 827.
[28] N.S. Chowdhury, D.K. Seth, M.G.B. Drew, S. Bhattacharya, Inorg. Chim. Acta 372 (2011) 183.
[29] M.P. Aarnts, D.J. Stufkens, M.P. Wilms, E.J. Baerends, A. Vlček Jr., I.P. Clark, M.W. George, J.J. Turner, Chem. Eur. J. 2 (1996) 1556.